Do Absorbing Aerosols or Scattering Aerosols Dominate the Impact of Aerosols on Ozone via Influencing Photolysis Rates?

Gao Jinhui[1], LI Ying[2], Xie Zhouqing[3], Wang Lili[4], Hu Bo[5], and Bao Fangwen[2]

[1]Chengdu University of Information Technology
[2]Southern University of Science and Technology
[3]University of Science and Technology of China
[4]Institute of Atmospheric Physics, Chinese Academy of Sciences
[5]State Key Laboratory of Atmospheric Boundary Layer Physics and Atmospheric Chemistry, Institute of Atmospheric Physics, Chinese Academy of Sciences

November 16, 2022

Posted on 16 Nov 2022 — CC-BY-NC-ND 4 — https://doi.org/10.1002/essoar.10508565.1 — This a preprint and has not been peer reviewed. Data may be preliminary.

Abstract

Since different optical properties, absorbing aerosols (AA) and scattering aerosols (SA) impact ozone differently via influencing photolysis rates. Notably, studies on the impact of SA have not reached a consistent conclusion, leading to disconfirmation regarding which type of aerosol dominates the impact of aerosols on ozone via influencing photolysis rates. Our results show that, in contrast to the decreasing impact of AA on ozone, SA decrease ozone chemical contribution (CHEM) near surface but increase that aloft, subsequently enhancing the vertical exchange of ozone and resulting the counteraction of the opposite vertical changes in CHEM. Consequently, ozone changed slightly, indicating that AA are the dominant aerosols. Reducing AA leads to ozone increase nonlinearly (ΔO_3). More than 86% of North China Plain could be covered by ΔO_3 when reducing more than 3/4 of AA. More attention should be paid on the balance between ozone and AA in determining synergetic control strategy.

Do Absorbing Aerosols or Scattering Aerosols Dominate the Impact of Aerosols on Ozone via Influencing Photolysis Rates?

Jinhui Gao[1,2,3], Ying Li[2,3*], Zhouqing Xie[4], Lili Wang[5], Bo Hu[5], Fangwen Bao[2,3]

[1]Plateau Atmosphere and Environment Key Laboratory of Sichuan Province, School of Atmospheric Sciences, Chengdu University of Information Technology, Chengdu, China.

[2]Department of Ocean Science and Engineering, Southern University of Science and Technology, Shenzhen, China.

[3]Center for the Oceanic and Atmospheric Science at SUSTech (COAST), Southern University of Science and Technology, Shenzhen, China.

[4]Department of Environmental Science and Engineering, University of Science and Technology of China, Hefei, China.

[5]State Key Laboratory of Atmosphere Boundary Layer Physics and Atmospheric Chemistry (LAPC), Institute of Atmospheric Physics, Chinese Academy of Sciences, Beijing, China.

*Corresponding author: Ying Li (liy66@sustech.edu.cn)

Key Points:

- Absorbing aerosols dominate the impact of aerosols on ozone via influencing photolysis rates.
- Scattering aerosols change chemical and physical contributions of ozone, changes offset with each other which finally impact ozone little.
- It shows quadratic relationship that reducing absorbing aerosols leads to nonlinear increase in surface ozone over the North China Plain.

Abstract

Since different optical properties, absorbing aerosols (AA) and scattering aerosols (SA) impact ozone differently via influencing photolysis rates. Notably, studies on the impact of SA have not reached a consistent conclusion, leading to disconfirmation regarding which type of aerosol dominates the impact of aerosols on ozone via influencing photolysis rates. Our results show that, in contrast to the decreasing impact of AA on ozone, SA decrease ozone chemical contribution (CHEM) near surface but increase that aloft, subsequently enhancing the vertical exchange of ozone and resulting the counteraction of the opposite vertical changes in CHEM. Consequently, ozone changed slightly, indicating that AA are the dominant aerosols. Reducing AA leads to ozone increase nonlinearly (ΔO_3). More than 86% of North China Plain could be covered by ΔO_3 when reducing more than 3/4 of AA. More attention should be paid on the balance between ozone and AA in determining synergetic control strategy.

Plain Language Summary

Aerosols can impact ozone via influencing photolysis rates. However, absorbing aerosols (AA) and scattering aerosols (SA) show different optical properties that impact ozone differently. It's noteworthy that previous studies on the impact of SA have not reached a consistent conclusion, leading to the disconfirmation of which type of aerosol dominates the impact of aerosols on ozone via influencing photolysis rates. In this study, we found that SA can decrease the chemical production of ozone (CHEM) near surface but significantly increase that aloft, then enhancing the vertical exchange of ozone. In this case, the strong vertical exchange neutralizes the opposite changes in CHEM and ultimately lead to very slight changes in ozone, suggesting AA dominates the impact of aerosols on ozone via influencing photolysis rates. It shows a quadratic relationship that reducing AA could lead to a nonlinear increase in surface ozone (ΔO_3). More than 86% of the North China Plain would experience ΔO_3 when reducing more than 3/4 of AA, especially in urban areas, the increment could be more than 5 ppb. Our results suggest that more attention should be paid on the balance between ozone and AA when determining the synergetic control policy of air quality in China.

1 Introduction

Air quality over the North China Plain (NCP) is suffered by high concentrations of aerosol and ozone in recent years (Zhang et al., 2014a; Gao et al., 2015; Ding et al., 2016; Cai et al., 2017; Lu et al., 2018; 2019; Dong et al., 2020; Li et al., 2020; Li et al., 2021). To improve the air quality, a series of stringent air quality control actions were implemented since 2013. With hard work during the following 5 years (from 2013 to 2017), the mean concentrations of particulate matter

with diameter less than 2.5 μm ($PM_{2.5}$) decreased by 33%, and this reduction even reached 38% in the Beijing-Tianjin-Hebei (BTH) region (Zhang et al., 2019). However, concentrations of surface ozone increased simultaneously (Lu et al., 2018; Liu & Wang, 2020a; 2020b), which was considered due to the decrease in aerosols (Li et al., 2019a; 2019b).

Light extinction of aerosols (including light absorption and scattering) can impact ozone via influencing the photolysis rates of ozone and its precursors, which has been studied worldwide in recent decades (Dickerson et al., 1997; Jacobson, 1998; Cartro et al., 2001; Li et al., 2005; Li et al., 2011; Gao et al., 2020). With continuous hard work, understanding of this mechanism is improving. However, there are still some unclear problems that need to be more sufficiently studied. It is well known that absorbing aerosols (AA) and scattering aerosols (SA) have different optical properties, and can influence photolysis rates differently, thus resulting in different impact on ozone (Dickerson et al., 1997; Jacobson, 1998; Liao et al., 1999). In this case, it is worth confirming which type of aerosol (AA or SA) dominates the impact of aerosols on ozone via influencing photolysis rates. And we believe that making this question clear can provide more information regarding the interactions between aerosols and ozone.

To solve this problem, it is necessary to confirm the influence of each type of aerosol on photolysis rates and the resulting impact on ozone. For AA, the conclusions of previous studies are consistent: the attenuation of incident solar irradiance induced by AA reduces photolysis rates and then weakens the photochemical production of ozone, and finally reduces surface ozone (Dickerson et al., 1997; He & Carmichael, 1999; Cartro et al., 2001; Li et al., 2005). However, most studies focused on the surface ozone but missed the impact on ozone throughout the entire planet boundary layer (PBL). Studies on the impact of SA on ozone have obtained different conclusions. Dickerson et al. (1997) reported that SA (for example, sulfate) could increase photolysis rates at higher altitudes, thus enhancing the ozone photochemical production and ultimately leading to the increase in ozone (with increases of 20 ppb or more). Other studies summarized the impact of SA differently. He and Carmichael (1999) reported that ozone showed only a slight increase induced by SA. Tie et al. (2005) reported that SA led to much smaller changes in ozone, and some other studies suggested that SA could cause ozone to increase and decrease simultaneously (Xing et al., 2017; Li et al., 2018). These different conclusions have resulted in large uncertainty regarding the impact of SA on ozone. Only by solving this uncertainly and clarifying the differences between the impacts of AA and SA can we reach our goal of determining the dominate aerosol impacting ozone via influencing photolysis rates.

In this study, the Weather Research and Forecasting model with Chemistry (WRF-Chem) was implemented to simulate air pollutants over the NCP in October 2018. By comparing the obtained results among the experiments, the impacts of AA and SA on ozone via influencing photolysis rates were quantitatively analyzed, respectively. Furthermore, by comparing the

impacts of the two aerosol types, the dominant aerosol in impacting ozone via influencing photolysis rates would be confirmed. Finally, the sensitivities of the changes in surface ozone caused by reducing the dominant aerosols over the NCP were also quantitatively discussed. Our results provide clearer insight into the impacts of aerosols on ozone and more scientific advice for synergistic control strategy regarding ozone and aerosols.

2 Methodology

2.1 Numerical simulation

To understand the impacts of the two types of aerosols on ozone through their influence on photolysis rates, we conducted numerical simulations with the WRF-Chem model (version 3.9.1.1, Skamarock et al., 2008; Grell et al., 2005). The model configurations are listed in the supporting information (SI: Test S1). All the aerosol species included in the applied aerosol scheme (Zaveri et al., 2008) were classified into AA or SA based on their refractive indexes (SI: Test S1 and Table S1). It should also be noted that the WRF-Chem model features two-way feedback that the impacts on ozone both via influencing photolysis rates and via affecting the development of the PBL (Gao et al., 2018) induced by the light extinction of aerosols can be included in this model system (SI: Fig. S2a). To isolate the impact of aerosols on ozone via influencing photolysis rates, some necessary modifications were made to the source codes of WRF-Chem to fulfill the purposes of this study. Detailed information about the model modifications can be found in the SI (Test S2 and Fig. S2b).

With the implementation of the modified WRF-Chem model, four experiments were established [SI: Test S3 (I) and Fig. S2b]: Exp1 was designed by considering the effects of all aerosols when calculating photolysis rates, it could be treated as base experiment and whose results could be used for the model evaluations. Exp2 was designed by not considering any effects of aerosols when calculating photolysis rates, and this experiment was treated as the blank experiment. Exp3 was designed by considering only the effect of SA when calculating photolysis rates, and Exp4 was designed by considering only the effect of AA when calculating photolysis rates. By comparing the results of these experiments, the differences of ozone between Exp2 and Exp3 show the impact of SA on ozone via influencing photolysis rates, and the differences of ozone between Exp2 and Exp4 show the impact of AA.

2.2 Model evaluation

The model performance was evaluated by comparing the simulations with observations of meteorological factors (temperature, wind speed and wind direction) and air pollutants (ozone, NO_2, and $PM_{2.5}$). As determined through a large number of comparisons, the model results matched well with the observations, suggesting that the model successfully reproduced the spatial and temporal variations of meteorology and air quality over the NCP during October 2018 (SI:

Test S4, Table S2, and fig. S3~S4). In addition, the observed photolysis rates ($J[NO_2]$ and $J[O_3{}^1D]$) and aerosol species (SO_4, NO_3, NH_4, BC, and OC) measured by the research group attached to the Institute of Atmospheric Physics (IAP) Chinese Academy of Sciences were also applied to evaluate the model performance in simulating the corresponding variables. By comparing the observations (Fig. S5~S8), our simulations captured the variations of these variables well. Especially during high aerosol episodes (i.e., 13^{th}-15^{th}, 20^{th}-22^{nd}, and 25^{th} in Oct. 2018), our results successfully captured the high concentrations of these aerosol species. In conclusion, the satisfactory model performances obtained for all the variables mentioned above indicated that the WRF-Chem model is capable of reproducing the atmospheric characteristics well over the NCP during Oct. 2018.

3 Results and discussions

3.1 Impacts on the photolysis rate profile and surface ozone

During the polluted days, the AA and SA vertical profiles (right panel of Fig. 1a) showed high concentrations within PBL but decreased significantly with altitude above the PBL (gray dashed line). The different optical properties of AA and SA resulted in different photolysis rate profiles. Taking $J[NO_2]$ as an example (left panel of Fig. 1a), $J[NO_2]$_clean (blue line) showed a vertical distribution without any impact from aerosols (as determined from the results of Exp2). When it was under the influence of AA, $J[NO_2]$_AA (red line) commonly decreased in the vertical direction due to the attenuation of solar irradiance caused by the light absorption of AA (Liao et al., 1999; Ding et al., 2016). This decreasing trend enlarged as altitude decreased, corresponding to the vertical distributions of AA concentrations. In contrast to AA, SA caused $J[NO_2]$_SA (green line) to decrease at lower altitudes but increase at higher altitudes. This was due to the backscattering effects of SA on solar irradiance leading to the attenuation of shortwave radiation at lower altitudes but the enhancement of shortwave radiation at higher altitudes (Dickerson et al., 1997; Liao et al., 1999). It should be noted $J[NO_2]$_SA was enhanced in the middle and upper layers of the PBL where ozone precursors (NOx and VOCs) exist. In this case, the enhanced photolysis rates may lead to stronger ozone photochemistry and increase the photochemical production of ozone. This is the key factor that led some previous studies to concluding that SA could result in an increase in ozone via influencing photolysis rates.

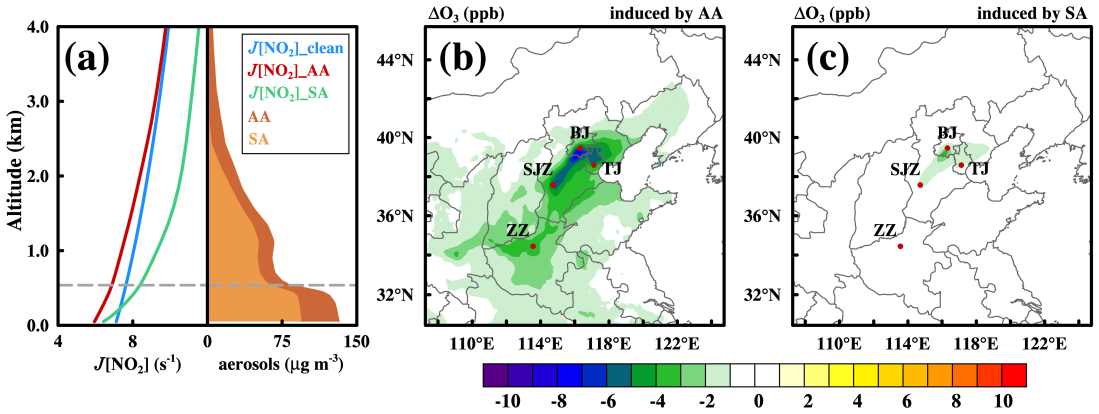

Figure 1. Mean profiles of J[NO_2] and different types of aerosols at Xianghe station at 12:00 in polluted days (a); mean distributions of the changes in surface ozone (ΔO_3) induced by AA (b) and SA (c) during the daytime (09:00~17:00 local time, LT) on polluted days. The gray dashed line in (a) denotes the planet boundary layer height (PBLH). The locations of the four representative cities are denoted as red dots in (b) and (c), BJ=Beijing, TJ=Tianjin, SJZ=Shijiazhuang, and ZZ=Zhengzhou.

By influencing photolysis rates, AA caused surface ozone to significantly decrease over the NCP region (Fig. 1b). This change in ozone (ΔO_3) showed a similar distribution to that of AA (Fig. S9a). And ΔO_3 was much more significant over urban areas (i.e., BJ, TJ, SJZ, and ZZ) where high concentrations of AA covered. For SA, our results differed from the significant increase in ozone reported by Dickerson et al. (1997), it showed that both values and coverage of ΔO_3 induced by SA were much less than those induced by AA (Fig .1c), although the SA concentrations were much higher than the AA concentrations (Fig. S9b). Thus, the result is consistent with the results of Tie et al. (2005) and Xing et al. (2017), who reported that SA leads to less significant changes in surface ozone through their influence on photolysis rates than AA. Hereby, it is clear that the two types of aerosols have different impacts on surface ozone, furthermore, how the impacts of the two aerosol types occur is worthy of more carefully studying.

3.2 Process analysis of the impacts on ozone induced by AA and SA

The impacts of aerosols on ozone can be reflected by the changes that occur in contributions to ozone development through chemical and physical processes (Gao et al., 2020). With the implementation of the process analysis (Zhang et al., 2014b; Gao et al., 2016), the mean change in each ozone contribution (chemistry, vertical mixing, and advection) induced by AA and SA over the four representative cities are presented in Fig. 2. Furthermore, by comparing these changes, the key factor that contributes the most to ΔO_3 can be determined.

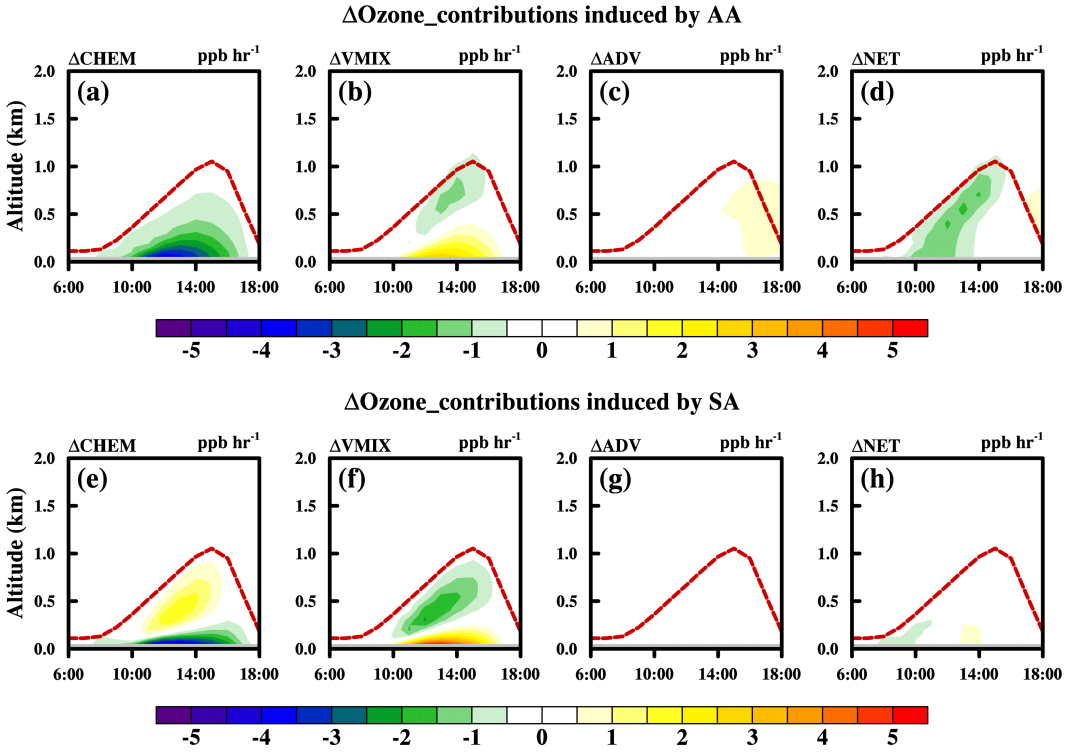

Figure 2. Average vertical distributions of the change in each process contribution induced by AA (a~d) and SA (e~h) as a function of time during daytime. The data is spatially sampled and averaged to represent the average situation among the four cities. ΔCHEM=change in chemistry, ΔVMIX=change in vertical mixing, ΔADV=change in advection, ΔNET=changes in the sum of these contributions. The red dashed lines denote the PBLH

Changes in each ozone contribution induced by AA are presented in Fig. 2a~2d. As a result of the decreased photolysis rates induced by AA, the ozone photochemistry was weakened, which showed the ozone contribution from chemistry (CHEM) decreased significantly in the PBL (as denoted by the negative ΔCHEM values in Fig. 2a), especially in the lower layers (Fig. 2a). Furthermore, ΔCHEM also enlarged the vertical ozone gradient. In this case, the turbulence within the PBL entrained more ozone aloft down to the surface, enhancing the contribution from vertical mixing (VMIX; Gao et al., 2020). Therefore, the ΔVMIX values were negative aloft but positive at lower altitudes (Fig. 2b). The contribution from advection (ADV) changed slightly, and ΔADV showed only small values in the afternoon (Fig. 2c). After summing all the changes (Fig. 2d), ΔNET showed a decrease in the entire PBL, suggesting that AA resulted in decreased ozone not only at the surface but also throughout the entire PBL. SA caused different changes in CHEM and VMIX. As shown in Fig. 2e, CHEM decreased at lower altitudes but increased significantly at higher altitudes in the PBL, corresponding to the influence on the photolysis rates induced by SA. ΔVMIX values induced by SA showed the same patterns as those induced by AA, but with a much

stronger intensity (Fig. 2f). ADV also showed little change in the PBL (Fig. 2g). Thus, SA also caused significant changes in both CHEM and VMIX. However, ΔCHEM and ΔVMIX showed opposite distributions with similar absolute values. As a result, ΔNET induced by SA showed very small values in the PBL (Fig. 2h), suggesting that SA caused much smaller changes in ozone in the entire PBL than AA, although very significant changes did occur in relevant chemical and physical processes.

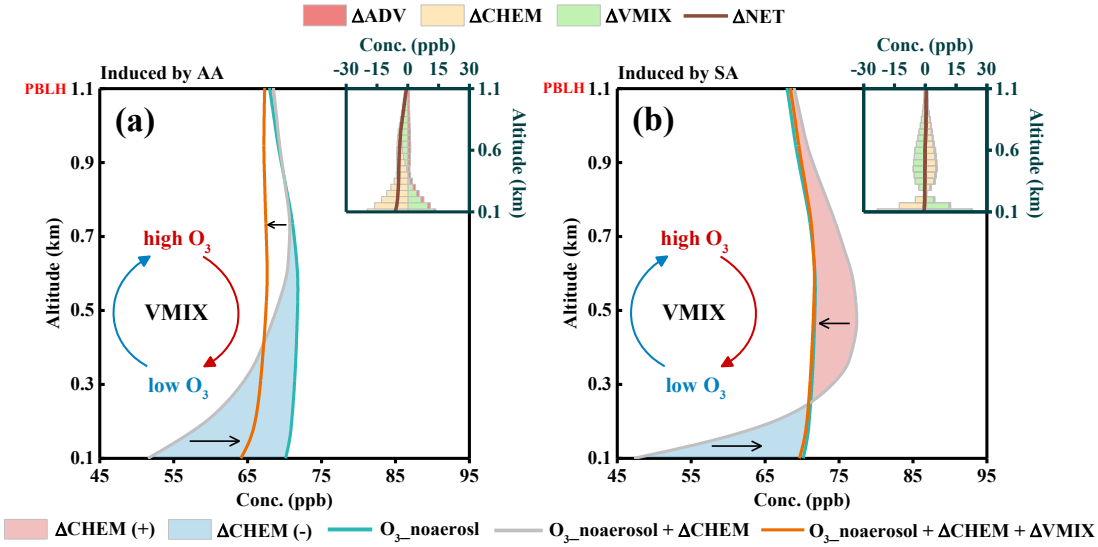

Figure 3. Synergy of ΔCHEM and ΔVMIX on ozone profile induced by AA and SA, respectively. ΔCHEM values are denoted by shading. Ozone profiles without the impact of aerosols (O_3_noaerosol) are denoted by green lines; ozone profiles impacted by ΔCHEM (O_3_noaerosol+ΔCHEM) are denoted by gray lines; and ozone profiles impacted by the synergy of ΔCHEM and ΔVMIX (O_3_noaerosol+ΔCHEM+ΔVMIX) are denoted by orange lines. The vertical budgets of the changes in ozone contributions induced by AA and SA are presented in the small panels at the top-right corners of (a) and (b), respectively.

Based on the discussion above, ΔCHEM and ΔVMIX are the two key factors that synergistically contribute to ΔO_3. Because of the different optical properties of AA and SA, the two types of aerosols caused CHEM and VMIX to change in different ways, ultimately leading to different changes in ozone in the PBL. Under the impact of AA (Fig. 3a), CHEM decreased in vertical direction, and the decrement was more significant at lower altitudes (light blue shades). In this case, ΔCHEM caused the ozone profile to form a greater vertical gradient (gray line) than that formed when ozone was not influenced by aerosols (green line). The greater vertical gradient could enhance the vertical exchange of ozone by entraining high concentrations of ozone aloft down to

the surface (as depicted in the schematic diagram on the left of Fig. 3a) till the vertical gradient was eliminated again. Due to the significant decrease in CHEM in the PBL, ozone in the lower layer was partly supplied by ozone aloft, and the final ozone profile (orange profile) still showed a decrease in the PBL. The budget of the changes in ozone contributions in vertical direction showed negative values, further suggesting the decrease in ozone within the PBL induced by AA (as shown in the small panel at the top-right corner of Fig. 3a). For SA (Fig. 3b), due to their influence on photolysis rates, CHEM increased at higher altitudes (pink shade) but decreased near the surface (light blue shade), causing the profile of ozone (gray line) to form a much more significant vertical gradient. This enhanced the vertical exchange of ozone with a strong intensity, which explained the occurrence of more significant ΔVMIX values induced by SA (Fig. 2f). More importantly, this vertical exchange resulted in the neutralization between the increase in CHEM at higher altitudes and the decrease in CHEM near the surface, finally leading to less obvious changes in ozone profile (orange line). And also, the budget of the changes in ozone contributions showed that ozone did not change significantly under the impact of SA. In addition, the different impacts of AA and SA on ozone obviously indicate that AA is the key factor dominating the impact of aerosols on ozone by influencing photolysis rates.

3.3 Sensitivity of the ΔO_3 caused by the reduction in AA

Our results suggested that ΔO_3 is more sensitive to AA. Hereby, taking the results from Exp1 as the base condition and comparing them with the results of four additional experiments [SI: Test S3 (II)] and Exp3, the sensitivities of ΔO_3 caused by the reduction in AA (by reducing AA by 1/4, 1/2, 3/4, 7/8, and entirely) over the NCP were examined in this section. Through the comparisons, surface ozone was found to increase as AA were reduced over the NCP (Fig. S10). As shown in Fig. 4a, when reducing AA by 1/4, ΔO_3 (with values of 1~2 ppb) covered only 9% of the NCP, mainly above Beijing, Tianjin and Hebei Province (Fig. S10a). When the reduction in AA increased to 1/2, the coverage of ΔO_3 significantly increased to 29.6×10^4 km^2 (58.1% of NCP), and the ΔO_3 increases were basically distributed in the range of 1~4 ppb. When AA was reduced by 3/4 or more, more than 86% of NCP was covered by ΔO_3. In addition, it is noteworthy that the greater the magnitude of the AA reduction was, the higher the resulting ΔO_3 values were. For example, when reducing all AA, 12.5% of the NCP was covered by ΔO_3 values greater than 5 ppb, and most of the increases were located above urban areas (i.e., BJ, TJ, SJZ and ZZ) that suffered by relatively high concentrations of AA (Fig. S9a).

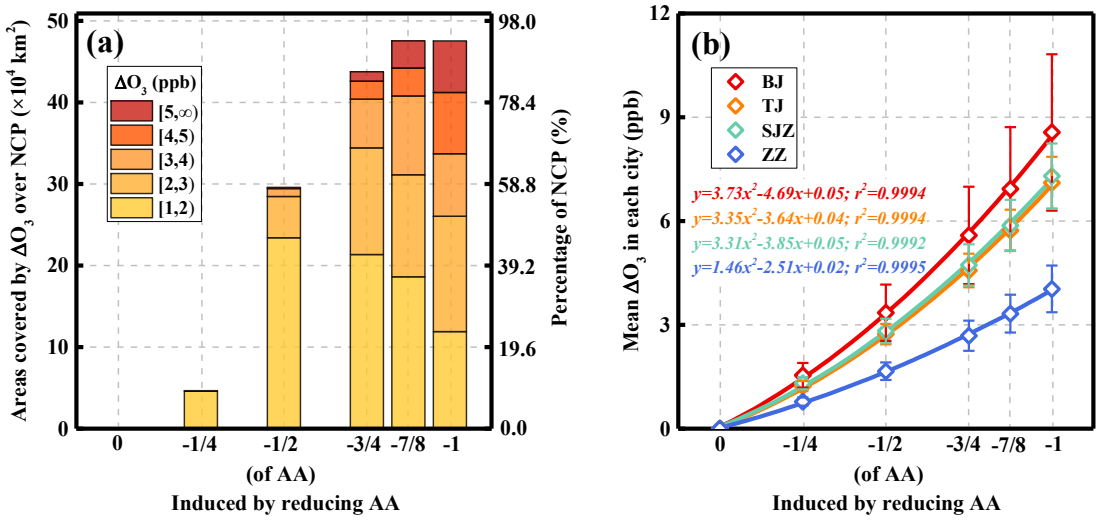

Figure 4. (a) Coverage of ΔO_3 at ground level induced by reducing AA over the NCP; (b) Trends of ΔO_3 induced by reducing AA in the four representative cities. For each city, data is spatial sampled and averaged.

The ΔO_3 trends induced by reducing AA in the four representative cities are presented in Fig. 4b. The mean ΔO_3 in BJ increased more significantly than those in the other cities. The maximum increment reached 8.6 ppb when reducing all AA. Second to BJ, the mean ΔO_3 values in TJ and SJZ showed similar trends, with maximum increments of 7.3 ppb and 7.1 ppb obtained when AA was reduced entirely. ΔO_3 values in ZZ increased the slowest, with a maximum increment of 4.0 ppb when AA was eliminated completely. Finally, it is noteworthy that the trends revealed a nonlinear relationship between ΔO_3 and the reduction in AA. And the nonlinear fitting lines obtained for each city indicated a quadratic relationship with high coefficient values (R^2>0.999). Basically, when the reduction in AA was equal to or greater than 3/4, ozone in BJ, TJ, and SJZ showed relatively high increments (≥5 ppb), suggesting that attention should be paid on the balance between ozone and reducing AA over the NCP, especially over the urban areas in the BTH region.

5 Conclusions

The impacts of aerosols on ozone by influencing photolysis rates have been widely discussed in previous studies, however, since different optical properties being shown on different aerosol types, ozone changes differently when it is impacted by AA and SA separately. And till now, there has been a lack of sufficient understanding regarding why and how these two types of aerosols impact surface ozone differently. In this study, the WRF-Chem model was implemented to simulate air pollutants over the NCP during Oct. 2018. By comparing the results of a series of well-designed experiments, the changes in ozone (ΔO_3) induced by AA and SA by influencing

290 photolysis rates were isolated, respectively. With the implementation of process analysis, the
291 impacts of the two types of aerosols on ozone were quantitatively discussed.

292 The different optical properties of AA and SA influenced photolysis rates differently, but
293 they both led to changes in CHEM and VMIX and thus synergistically contributed to ΔO_3 in the
294 PBL. For AA, decreased photolysis rates weakened the photochemistry of ozone in the PBL, which
295 ultimately decreased CHEM in the PBL. This decrease in CHEM also enlarged the vertical
296 gradient of ozone and then resulted in the enhancement of VMIX, causing more ozone aloft being
297 entrained downward and partly offset the decrease in ozone at the surface. As a result, ozone was
298 decreased in the entire PBL induced by AA. This synergy between CHEM and VMIX also
299 dominated the impact of SA, but different variations were caused by the scattering effect of SA on
300 solar irradiance. The scattering effect of SA decreased the photolysis rates near surface but
301 enhanced which in the middle and upper layers of the PBL. Correspondingly, CHEM decreased
302 near surface but increased significantly in the middle and upper layers of the PBL. The changes in
303 CHEM formed a more significant vertical gradient that enhanced the vertical exchange of ozone.
304 In this case, the vertical exchange neutralized the decrement of CHEM near surface, which was
305 counteracted by the increment of CHEM aloft, ultimately resulting in the ozone showing much
306 smaller changes than those induced by AA.

307 Since ozone is more sensitive to AA than SA, the sensitivity of ΔO_3 caused by the reduction
308 in AA over the NCP was examined. When AA were reduced by 1/4, only approximately 9% of
309 the NCP was covered by ΔO_3 with values of 1~2 ppb. The coverage of ΔO_3 increased dramatically
310 (58.1%) when the reduction in AA increased to 1/2. And when reducing AA by more than 3/4,
311 more than 86% of the NCP was covered by ΔO_3, suggesting that the reduction in AA can lead to
312 a significant increase in ozone. In addition, ΔO_3 was relatively high over the urban areas that
313 suffered by high concentrations of AA. Basically, it showed a quadratic relationship between ΔO_3
314 and the reduction in AA. When the reduction in AA was equal to or greater than 3/4, ozone
315 increased by more than 5 ppb in BJ, TJ, and SJZ, suggesting that attention should be paid on the
316 balance between ozone and AA when conducting the air quality control actions in the NCP,
317 especially in the urban areas of the BTH region. Our results provide quantitative evidence for the
318 synergetic control strategy of aerosols and ozone in the NCP region and even across China.

319

320 **Acknowledgments**

321 This work was supported by the National Natural Science Foundation of China (Grant no.
322 41961160728), Shenzhen Science and Technology Program (KQTD20180411143441009), Key-
323 Area Research and Development Program of Guangdong Province (2020B1111360001),
324 Guangdong Basic and Applied Basic Research Fund Committee (2020B1515130003), Key

Special Project for Introduced Talents Team of Southern Marine Science and Engineering Guangdong Laboratory (Guangzhou) (GML2019ZD0210), National Natural Science Foundation of China (Grant no. 41905114, 42105124, 41575106), Shenzhen Key Laboratory Foundation (ZDSYS20180208184349083), Center for Computational Science and Engineering at Southern University of Science and Technology. Observations can be access

Open Research

Data availability statement. We have uploaded all the data used in this study to Zenodo. It is available at https://zenodo.org/record/5606501#.YXpOr9lBz1I

References

Castro, T., Madronich, S., Rivale, S., Muhlia, A., & Mar, B. (2001). The influence of aerosols on photochemical smog in Mexico City. *Atmospheric Environment, 35*(10), 1765-1772. doi: 10.1016/S1352-2310(00)00449-0

Cai, W. J., Li, K., Liao, H., Wang, H. J., & Wu, L. X. (2017). Weather conditions conducive to Beijing severe haze more frequent under climate change. *Nature Climate Change, 7*(4), 257-263. doi:10.1038/Nclimate3249

Dickerson, R. R., Kondragunta, S., Stenchikov, G., Civerolo, K. L., Doddridge, B. G., & Holben, B. N. (1997). The impact of aerosols on solar ultraviolet radiation and photochemical smog. *Science, 278*(5339), 827-830. doi: 10.1126/science.278.5339.827

Ding, A. J., Huang, X., Nie, W., Sun, J. N., Kerminen, V. M., Petaja, T., et al. (2016). Enhanced haze pollution by black carbon in megacities in China. *Geophysical Research Letters, 43*(6), 2873-2879. doi:10.1002/2016GL067745

Dong, Y. M., Li, J., Guo, J. P., Jiang, Z. J., Chu, Y. Q., Chang, L., et al. (2020). The impact of synoptic patterns on summertime ozone pollution in the North China Plain. *Science Of the Total Environment, 735*, 139559. doi: 10.1016/j.scitotenv.2020.139559

Gao, J. H., Zhu, B., Xiao, H., Kang, H. Q., Hou, X. W., & Shao, P. (2016). A case study of surface ozone source apportionment during a high concentration episode, under frequent shifting wind conditions over the Yangtze River Delta, China. *Science of the Total Environment, 544*, 853-863. doi:10.1016/j.scitotenv.2015.12.039

Gao, J. H., Zhu, B., Xiao, H., Kang, H. Q., Pan, C., Wang, D. D., et al. (2018). Effects of black carbon and boundary layer interaction on surface ozone in Nanjing, China. *Atmospheric Chemistry and Physics, 18*(10), 7081-7094. doi:10.5194/acp-18-7081-2018

Gao, J. H., Li, Y., Zhu, B., Hu, B., Wang, L. L., & Bao, F. W. (2020). What have we missed when studying the impact of aerosols on surface ozone via changing photolysis rates?

Atmospheric Chemistry and Physics, 20(18), 10831-10844. doi:10.5194/acp-20-10831-2020

Gao, M., Guttikunda, S. K., Carmichael, G. R., Wang, Y. S., Liu, Z. R., Stanier, C. O., et al. (2015). Health impacts and economic losses assessment of the 2013 severe haze event in Beijing area. *Science of the Total Environment, 511*, 553-561. doi:10.1016/j.scitotenv.2015.01.005

Grell, G. A., Peckham, S. E., Schmitz, R., McKeen, S. A., Frost, G., Skamarock, W. C., et al. (2005). Fully coupled "online" chemistry within the WRF model, *Atmospheric Environment*, *39*, 6957-6975. doi: 10.1016/j.atmosenv.2005.04.027

He, S., & Carmichael, G. R. (1999). Sensitivity of photolysis rates and ozone production in the troposphere to aerosol properties. *Journal of Geophysical Research-Atmospheres, 104*(D21), 26307-26324. doi: 10.1029/1999jd900789

Jacobson, M. Z. (1998). Studying the effects of aerosols on vertical photolysis rate coefficient and temperature profiles over an urban airshed. *Journal Of Geophysical Research-Atmospheres, 103*(D9), 10593-10604. doi: 10.1029/98jd00287

Li, G. H., Zhang, R. Y., Fan, J. W., & Tie, X. X. (2005). Impacts of black carbon aerosol on photolysis and ozone. *Journal of Geophysical Research-Atmospheres, 110*(D23). doi: D2320610.1029/2005jd005898

Li, J., Wang, Z., Wang, X., Yamaji, K., Takigawa, M., Kanaya, Y., et al. (2011). Impacts of aerosols on summertime tropospheric photolysis frequencies and photochemistry over Central Eastern China. *Atmospheric Environment, 45*(10), 1817-1829. doi:10.1016/j.atmosenv.2011.01.016

Li, J., Chen, X. S., Wang, Z. F., Du, H. Y., Yang, W. Y., Sun, Y. L., et al. (2018). Radiative and heterogeneous chemical effects of aerosols on ozone and inorganic aerosols over East Asia. *Science of the Total Environment, 622*, 1327-1342. doi:10.1016/j.scitotenv.2017.12.041

Li, K., Jacob, D. J., Liao, H., Shen, L., Zhang, Q., & Bates, K. H. (2019a). Anthropogenic drivers of 2013-2017 trends in summer surface ozone in China. *Proceedings Of the National Academy of Sciences, 116*(2), 422-427. doi:10.1073/pnas.1812168116

Li, K., Jacob, D. J., Liao, H., Zhu, J., Shah, V., Shen, L., et al. (2019b). A two-pollutant strategy for improving ozone and particulate air quality in China. *Nature Geoscience, 12*(11), 906-910. doi:10.1038/s41561-019-0464-x

Li, K., Jacob, D. J., Shen, L., Lu, X., De Smedt, I., & Liao, H. (2020). Increases in surface ozone pollution in China from 2013 to 2019: anthropogenic and meteorological influences. *Atmospheric Chemistry and Physics, 20*(19), 11423-11433. doi:10.5194/acp-20-11423-2020

Li, K., Jacob, D. J., Liao, H., Qiu, Y., Shen, L., Zhai, S., et al. (2021). Ozone pollution in the North China Plain spreading into the late-winter haze season. *Proceedings of the National Academy of Sciences, 118*(10), e2015797118. doi:10.1073/pnas.2015797118

Liao, H., Yung, Y. L., & Seinfeld, J. H. (1999). Effects of aerosols on tropospheric photolysis rates in clear and cloudy atmospheres. *Journal of Geophysical Research-Atmospheres, 104*(D19), 23697-23707. doi: 10.1029/1999jd900409

Liu, Y. M., & Wang, T. (2020a). Worsening urban ozone pollution in China from 2013 to 2017-Part 1: The complex and varying roles of meteorology. *Atmospheric Chemistry and Physics, 20*(11), 6305-6321. doi:10.5194/acp-20-6305-2020

Liu, Y. M., & Wang, T. (2020b). Worsening urban ozone pollution in China from 2013 to 2017-Part 2: The effects of emission changes and implications for multi-pollutant control. *Atmospheric Chemistry and Physics, 20*(11), 6323-6337. doi:10.5194/acp-20-6323-2020

Lu, X., Hong, J. Y., Zhang, L., Cooper, O. R., Schultz, M. G., Xu, X. B., et al. (2018). Severe Surface Ozone Pollution in China: A Global Perspective. *Environmental Science & Technology Letters, 5*(8), 487-494. doi:10.1021/acs.estlett.8b00366

Lu, X., Zhang, L., Chen, Y. F., Zhou, M., Zheng, B., Li, K., et al. (2019). Exploring 2016-2017 surface ozone pollution over China: source contributions and meteorological influences. *Atmospheric Chemistry and Physics, 19*(12), 8339-8361. doi:10.5194/acp-19-8339-2019

Skamarock, W., Klemp, J. B., Dudhia, J., Gill, D. O., Barker, D. M., Duda, M., et al. (2008). A description of the advanced research WRF version 3, NCAR technical note NCAR/TN/u2013475

Tie, X. X., Madronich, S., Walters, S., Edwards, D. P., Ginoux, P., Mahowald, N., et al. (2005). Assessment of the global impact of aerosols on tropospheric oxidants. *Journal of Geophysical Research-Atmospheres, 110*(D3). doi: D0320410.1029/2004jd005359

Xing, J., Wang, J. D., Mathur, R., Wang, S. X., Sarwar, G., Pleim, J., et al. (2017). Impacts of aerosol direct effects on tropospheric ozone through changes in atmospheric dynamics and photolysis rates. *Atmospheric Chemistry and Physics, 17*(16), 9869-9883. doi:10.5194/acp-17-9869-2017

Zaveri, R. A., Easter, R. C., Fast, J. D. & Peters, L. K. (2008). Model for simulating aerosol interactions and chemistry (MOSAIC), *Journal of Geophysical Research-Atmospheres*, *113*, D13204. doi: 10.1029/2007jd008782

Zhang, J. K., Sun, Y., Liu, Z. R., Ji, D. S., Hu, B., Liu, Q., et al. (2014a). Characterization of submicron aerosols during a month of serious pollution in Beijing, 2013. *Atmospheric Chemistry and Physics, 14*(6), 2887-2903. doi:10.5194/acp-14-2887-2014

Zhang, H., DeNero, S. P., Joe, D. K., Lee, H. H., Chen, S. H., Michalakes, J. et al. (2014b). Development of a source oriented version of the WRF/Chem model and its application to

the California regional PM_{10}/$PM_{2.5}$ air quality study, *Atmospheric Chemistry And Physics.*, *14*, 485-503. doi: 10.5194/acp-14-485-2014

Zhang, Q., Zheng, Y. X., Tong, D., Shao, M., Wang, S. X., Zhang, Y. H., et al. (2019). Drivers of improved PM2.5 air quality in China from 2013 to 2017. *Proceedings Of the National Academy of Sciences, 116*(49), 24463-24469. doi:10.1073/pnas.1907956116

Geophysical Research Letters

Supporting Information for

Do Absorbing Aerosols or Scattering Aerosols Dominate the Impact of Aerosols on Ozone via Influencing Photolysis Rates?

Jinhui Gao[1,2,3], Ying Li[2,3*], Zhouqing Xie[4], Lili Wang[5], Bo Hu[5], Fangwen Bao[2,3]

[1]Plateau Atmosphere and Environment Key Laboratory of Sichuan Province, School of Atmospheric Sciences, Chengdu University of Information Technology, Chengdu, China.

[2]Department of Ocean Science and Engineering, Southern University of Science and Technology, Shenzhen, China.

[3]Center for the Oceanic and Atmospheric Science at SUSTech (COAST), Southern University of Science and Technology, Shenzhen, China.

[4]Department of Environmental Science and Engineering, University of Science and Technology of China, Hefei, China.

[5]State Key Laboratory of Atmosphere Boundary Layer Physics and Atmospheric Chemistry (LAPC), Institute of Atmospheric Physics, Chinese Academy of Sciences, Beijing, China.

Contents of this file

Introduction

In this supporting information, we list the additional texts, tables, and figures to support our study. To be specific, (1) the model configuration and aerosol classification are introduced by text S1, figure S1, and table S1; (2) the model modification is introduced by text S2, and figure S2; (3) the experiments design is given by text S3 and figure S2; (4) for model evaluation, please check text S4, table S2, and figure S4~S8; (5) mean distributions of absorbing aerosols (AA) and scattering aerosols (SA) at the ground level during daytime is shown in figure S9; (6) mean distributions of ΔO_3 induced by the reduction of AA is shown in figure S10.

Text S1: Model configuration and Aerosol classification.

The Weather Research and Forecasting with Chemistry (WRF-Chem) model (version 3.9.1.1) was implemented in this study which has been widely used to study the air quality problems worldwide. Regarding the model configurations, the model domains (fig. S1), spatial-temporal resolutions, and selected parameterizations are just as the same as which in our previous work and detailed information can be checked in Gao et al. (2020).

The Model for Simulating Aerosol Interactions and Chemistry with eight bins (MOSAIC-8bins; Zaveri et al., 2008) is chosen as the aerosol chemistry scheme, which includes eight chemical species: Sulfate (SO_4), Nitrate (NO_3), Ammonium (NH_4), Sodium (Na), Chlorine (Cl), Organic Carbon (OC), Black Carbon (BC), and Other Inorganics aerosols (OIN). Based on the refractive index of each species (Table S1), the eight aerosol species were classified into absorbing aerosols (AA) and scattering aerosols (SA). BC is a typical AA. Second to BC, OIN is also treated as AA since relevant greater imaginary part than other species (excluding BC). The other aerosol species (SO_4, NO_3, NH_4, Na, Cl, and OC) are treated as SA since the extremely approaching zero of the imaginary parts.

Text S2: Model modification.

The WRF-Chem model, composed by meteorology part and chemistry part (Skamarock et al., 2008; Grell et al., 2005), is featured by the two-way feedback. At each time step, the results of the meteorology part drive the chemistry part, meanwhile the results of the chemistry part can feedback the meteorology part via multiple ways, for example the radiation feedback of aerosols (Liao & Seinfeld, 2005; Fan et al., 2015). Thus, by implementing this model system, the impacts of aerosols on ozone via influencing photolysis rates and via affecting the development of the planet boundary layer (PBL) (Gao et al., 2018) induced by aerosols are included in this model system. To isolate the impact of aerosols on ozone via influencing photolysis rates, some necessary modifications were conducted to the source codes of WRF-Chem (fig. S2). To be specific, another set of variables associated with the optical properties of aerosols were identified in the WRF-Chem model system (for example, tauaer1~4, represent the aerosol optical depth at spectrum 1~4; extaer1~4, represent the extinction coefficient of aerosols at spectrum 1~4).

The additional variables were calculated by the specified aerosols we chose. For example, when all the aerosols were input, they equal to the original variables; and when AA (or SA) were input, they represented the optical properties of AA (or SA). As shown in fig. S2b, the additional variables (red flow) took part in the calculations of photolysis rates, meanwhile, the calculations of radiation still used the original variables (blue flow) and would not disturb the radiation feedback of aerosols which kept the same effect with the original WRF-Chem did. By controlling the additional variables via choosing different types of aerosols, the photolysis rates can be changed but the radiation feedback of aerosols will not be changed. Therefore, the impact of aerosols on ozone via influencing photolysis rates can be isolated.

Text S3: Experiments design.

(I) According to the modified WRF-Chem, four experiments were established (fig. S2): Exp1 is designed by considering the effects of all the aerosols when the model system doing the calculation of photolysis rates, and Exp1 can be treated as the base experiment whose results can be used for the model validation; Exp2 is designed by not considering any effects of aerosols when doing the calculation of photolysis rates which can be treated as the blank experiment; Exp3 is designed by only considering the effect of SA when doing the photolysis rates calculations; and Exp4 is designed by only considering the effect of AA when doing the photolysis rates calculations. By comparing the results from the experiments, the differences of the ozone concentrations between Exp2 and Exp3 show the impact of SA on ozone via influencing the photolysis rates. While the differences of ozone concentrations between Exp2 and Exp4 show the impact of AA.

(II) In order to examine the sensitivity of the changes of surface ozone caused by the reduction of AA, four additional experiments were designed with the implementation of the modified WRF-Chem. When doing the calculations of photolysis rates, keeping the SA just as the same as which in Exp1, reducing 1/4 (Exp5), 1/2 (Exp6), 3/4 (Exp7), and 7/8 (Exp8) of AA, respectively. And for Exp3, the results also represented the conditions of reducing all AA. Comparing the results from these experiments with which from Exp1, the changes of surface ozone induced by reducing different levels of AA can be presented, respectively.

Text S4: Model evaluation

Since the same model configurations with which in our previous study (Gao et al., 2020), the model performances on meteorological factors (temperature, wind speed and wind direction), air pollutants (ozone, NO_2, and $PM_{2.5}$) had been evaluated by comparing large quantities of observations from hundreds of stations distributed in eastern China (fig. S1b). And according to the statistical metrics (fig. S3~S4, and table S2), it showed that the simulations and observations agreed very well with each other for both the meteorological factors and the air pollutants which also suggested that our simulations well captured the spatial and temporal variations of meteorology and air pollutants over the North China Plain (NCP) in Oct. 2018. The simulated $J[NO_2]$ and $J[O_3{}^1D]$ were also compared with the

observed data. The observations were measured at the station located in Xianghe, Hebei province, which attached to the Institute of Atmospheric Physics (IAP) Chinese Academy of Sciences. Our simulations well captured the variations of the time series of two photolysis rates, especially the low values occurred during the three high aerosol episodes (13^{th}~15^{th}, 20^{th}~22^{nd}, and 25^{th} in Oct. 2018, detailed information also can be checked in Gao et al., 2020). In addition, aerosol species also should be validated since much attention being focused on the different impacts of AA and SA in this study. Thus, we collected the daily averaged concentrations of five aerosol species (NH_4, NO_3, SO_4, OC and BC) measured at three cities (Beijing, Tianjin, and Baoding) which being used for evaluating the capability of WRF-Chem in simulating aerosols species. By comparing the observations (Figure S6~S8), the simulated data was very close to the observations and our result basically reproduced the pattern of each aerosol species, especially for NH_4, SO_4, and NO_3. For example, our simulations well captured the high concentrations of the aerosol species occurring in the aerosol episodes in each city (i.e., 13^{th}-15^{th}, 20^{th}-22^{nd}, and 25^{th} in Oct. 2018). And when the concentrations of the observations were low, our simulations also agreed well with the observations. In conclusion, the satisfied model performances on all the variables mentioned above indicate that WRF-Chem model system is capable to reproduce the features of atmosphere (both meteorology and air quality) over NCP during Oct. 2018.

References:

Fan, J., Rosenfeld, D., Yang, Y., Zhao, C., Leung, L. R., & Li, Z. (2015). Substantial contribution of anthropogenic air pollution to catastrophic floods in Southwest China, *Geophysical Research Letters, 42*(14), 6066-6075. doi:10.1002/2015GL064479

Gao, J. H., Li, Y., Zhu, B., Hu, B., Wang, L. L., & Bao, F. W. (2020). What have we missed when studying the impact of aerosols on surface ozone via changing photolysis rates? *Atmospheric Chemistry and Physics*, *20*(18), 10831-10844. doi:10.5194/acp-20-10831-2020

Grell, G. A., Peckham, S. E., Schmitz, R., McKeen, S. A., Frost, G., Skamarock, W. C., et al. (2005). Fully coupled "online" chemistry within the WRF model, *Atmospheric Environment*, *39*, 6957-6975. doi:10.1016/j.atmosenv.2005.04.027

Liao, H., & Seinfeld, J. (2005). Global impacts of gas-phase chemistry-aerosol interactions on direct radiative forcing by anthropogenic aerosols and ozone, *Journal Of Geophysical Research-Atmospheres*, *110*, D18. doi:10.1029/2005JD005907

Skamarock, W., Klemp, J. B., Dudhia, J., Gill, D. O., Barker, D. M., Duda, M., et al. (2008). A description of the advanced research WRF version 3, NCAR technical note NCAR/TN/u2013475

Zaveri, R. A., Easter, R. C., Fast, J. D. & Peters, L. K. (2008). Model for simulating aerosol interactions and chemistry (MOSAIC), *Journal of Geophysical Research-Atmospheres*, *113*, D13204. doi:10.1029/2007jd008782

Figure S1. Two nested domains for numerical simulation. Locations of the observation stations are presented in (b).

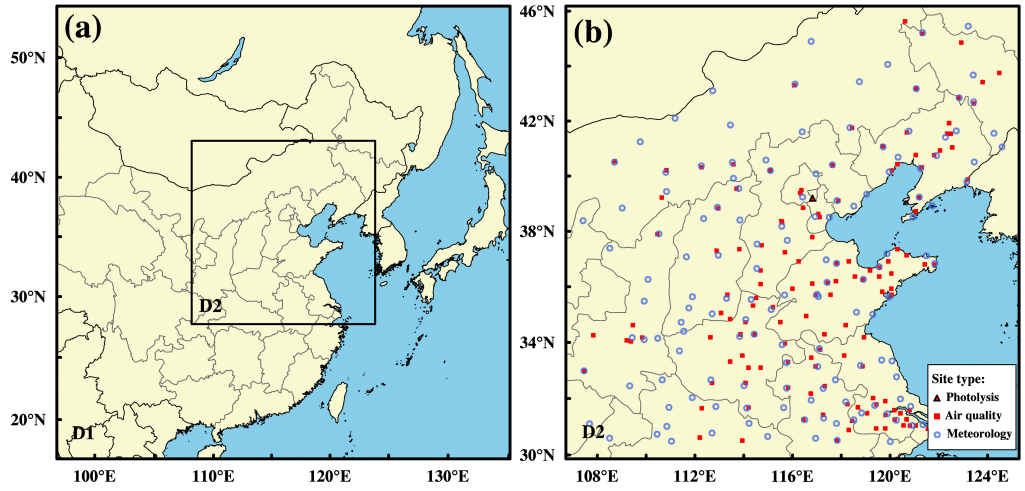

Figure S2. Flow charts of the original WRF-Chem (a) and the modified WRF-Chem (b). The experiments design is also presented in (b).

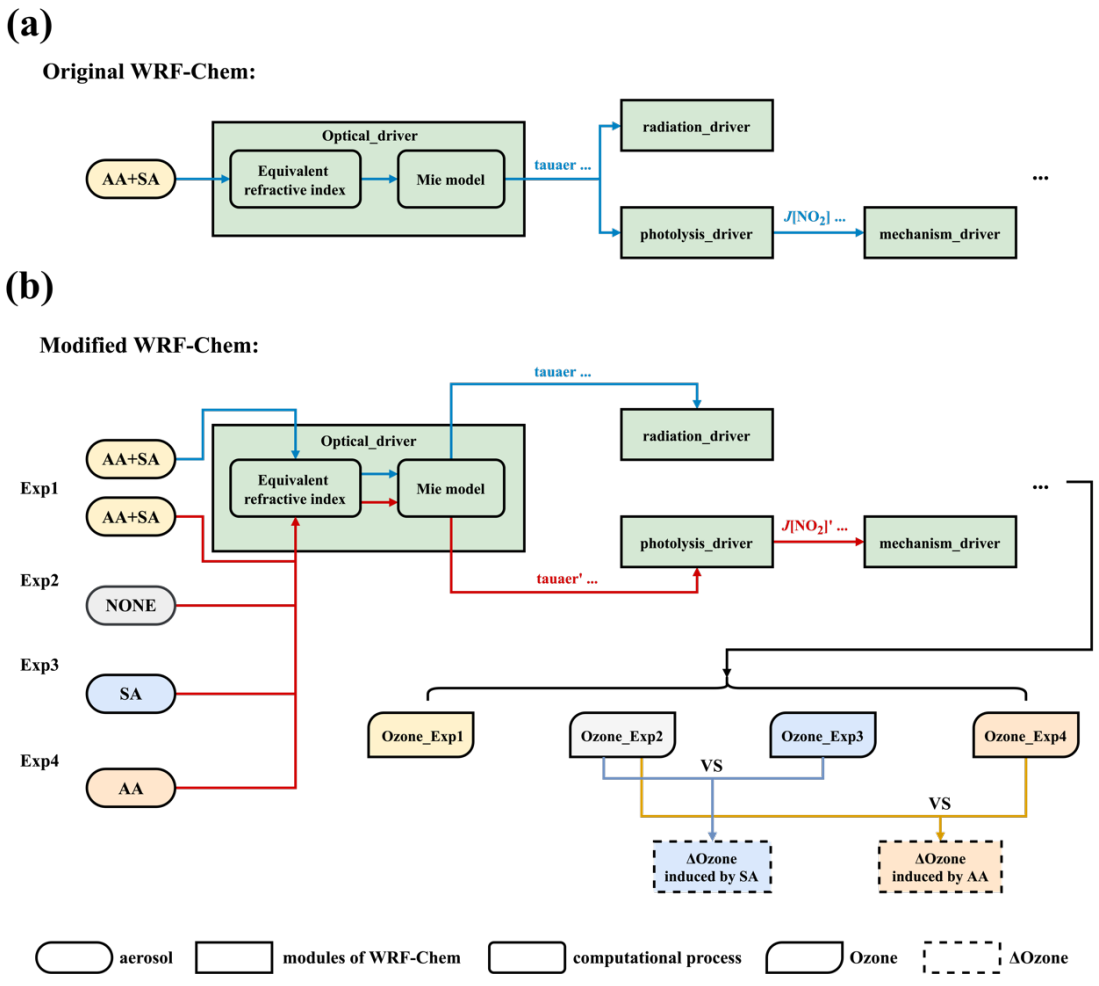

Figure S3. Taylor diagram for displaying model performance metrics on meteorological factors: (a) Temperature at 2m above surface; (b) Wind speed; (c) Wind direction. The radial distance from origin represents the Normalized Mean Error (NME); the azimuthal position represents the Index of Agreement (IOA); triangles represent the Normalized Mean Bias (NMB), over- and under-estimation are denoted as red up-triangle and blue down-triangle, respectively.

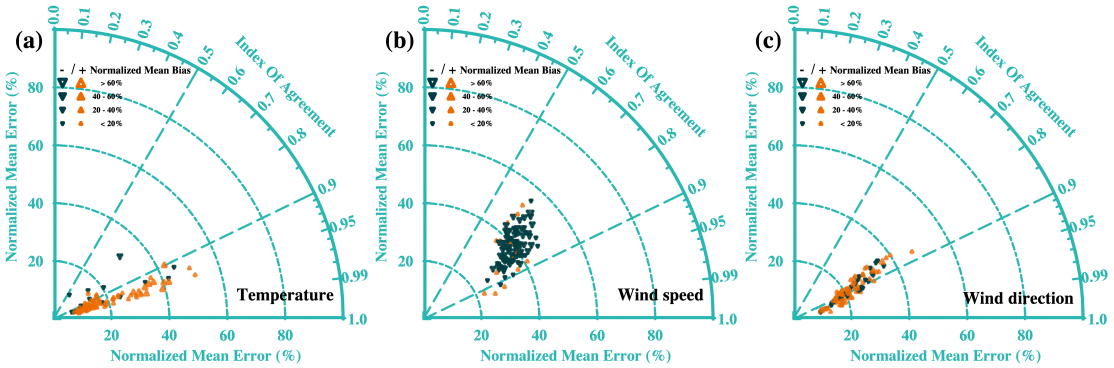

Figure S4. Same to figure S3 but for air pollutants: (a) Ozone; (b) NO_2; (c) $PM_{2.5}$.

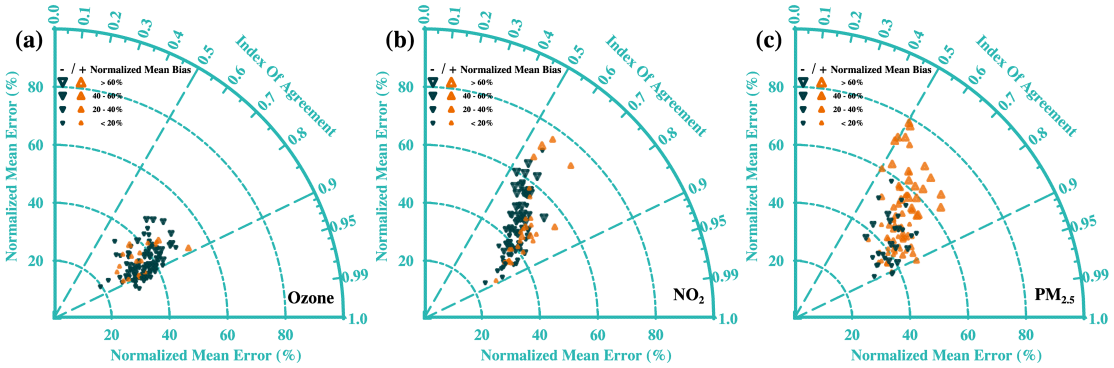

Figure S5. Comparisons of photolysis rates (a, $J[NO_2]$; b, $J[O_3{}^1D]$) between simulations and observations at Xianghe Station.

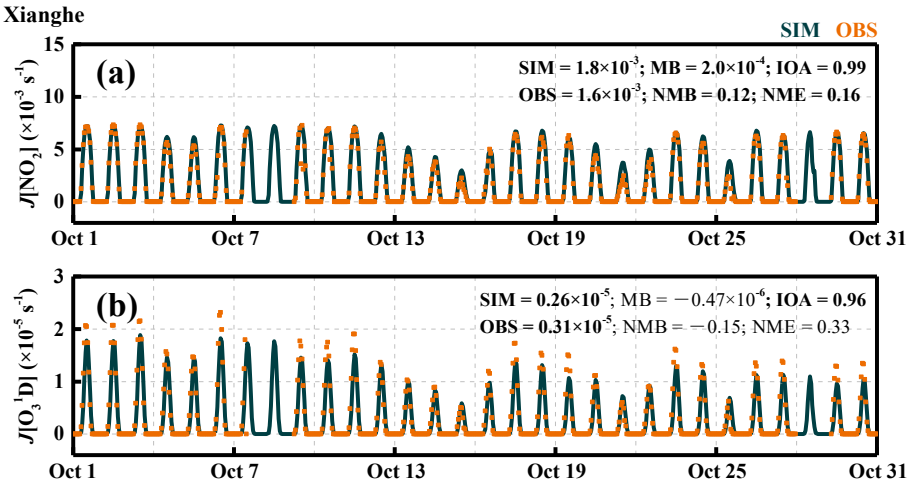

Figure S6. Comparisons of the chemical species of aerosols between simulations and observations in Beijing.

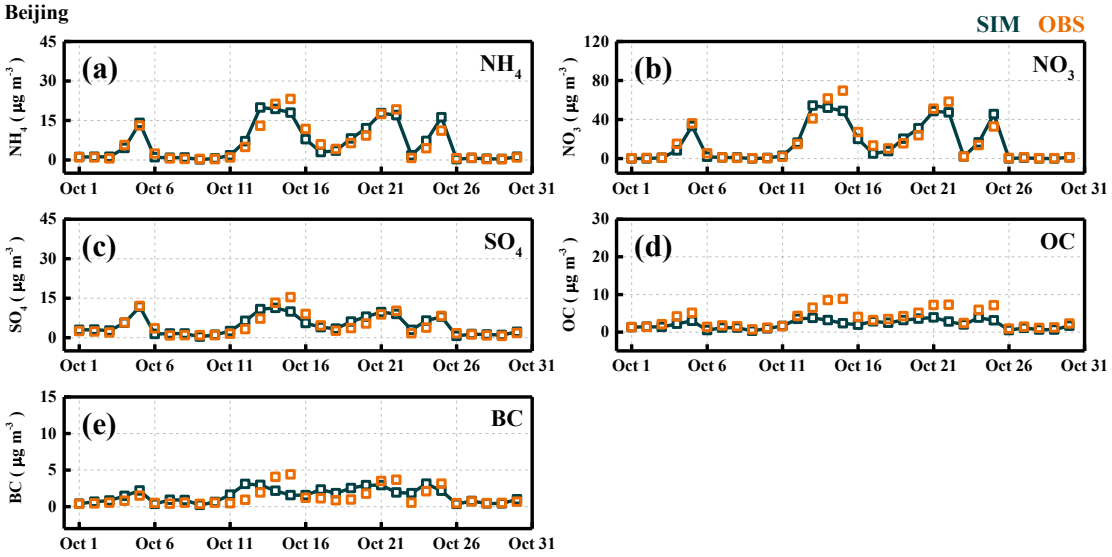

Figure S7. Same to figure S6, but in Tianjin.

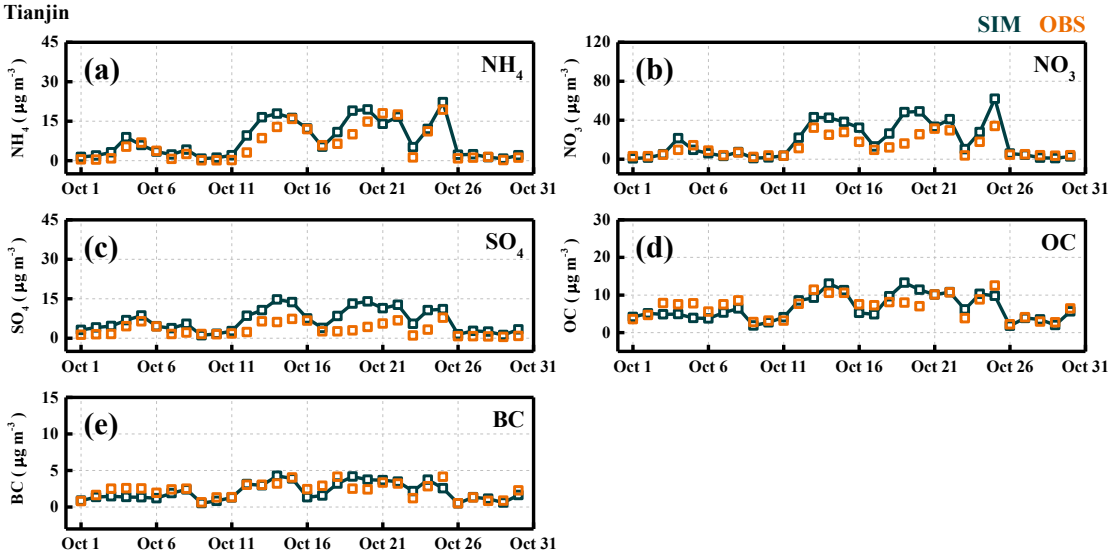

Figure S8. same to figure S6, but in Baoding.

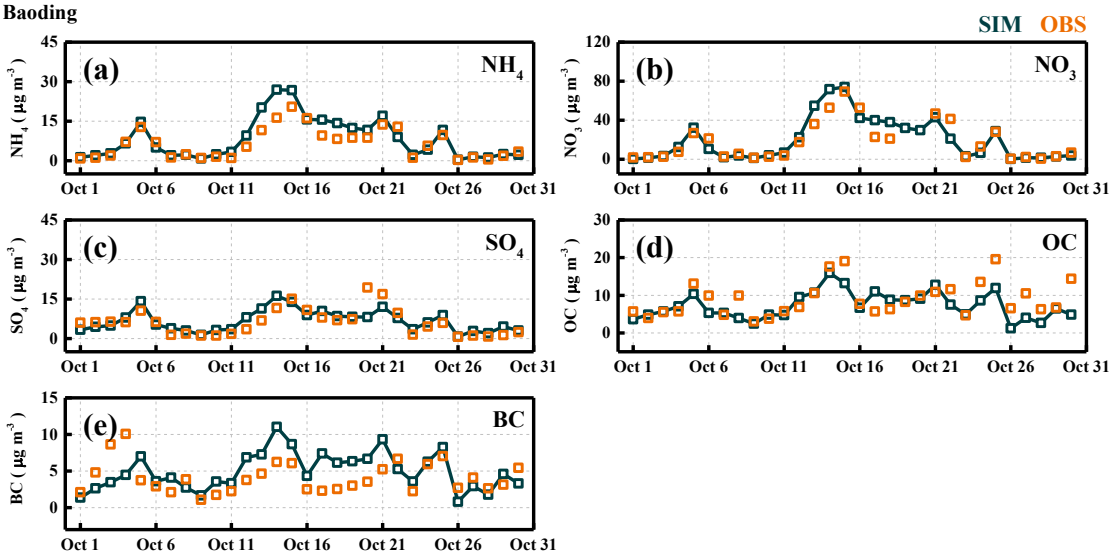

Figure S9. Mean distributions of AA and SA at the ground level during daytime (09:00~17:00 local time) in polluted days of Oct. 2018.

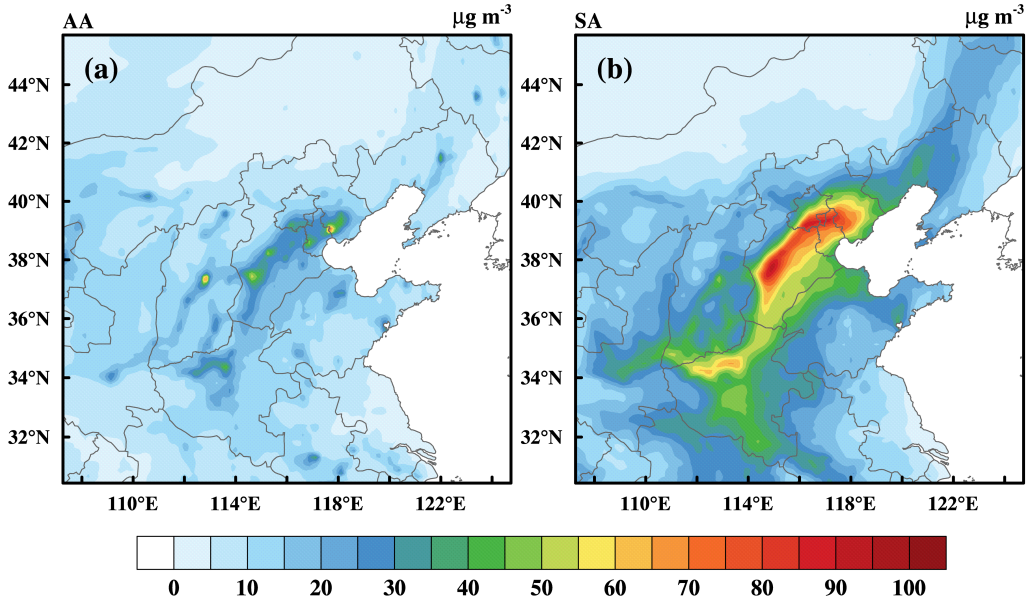

Figure S10. Mean distributions of ΔO_3 induced by different reduction levels of AA.

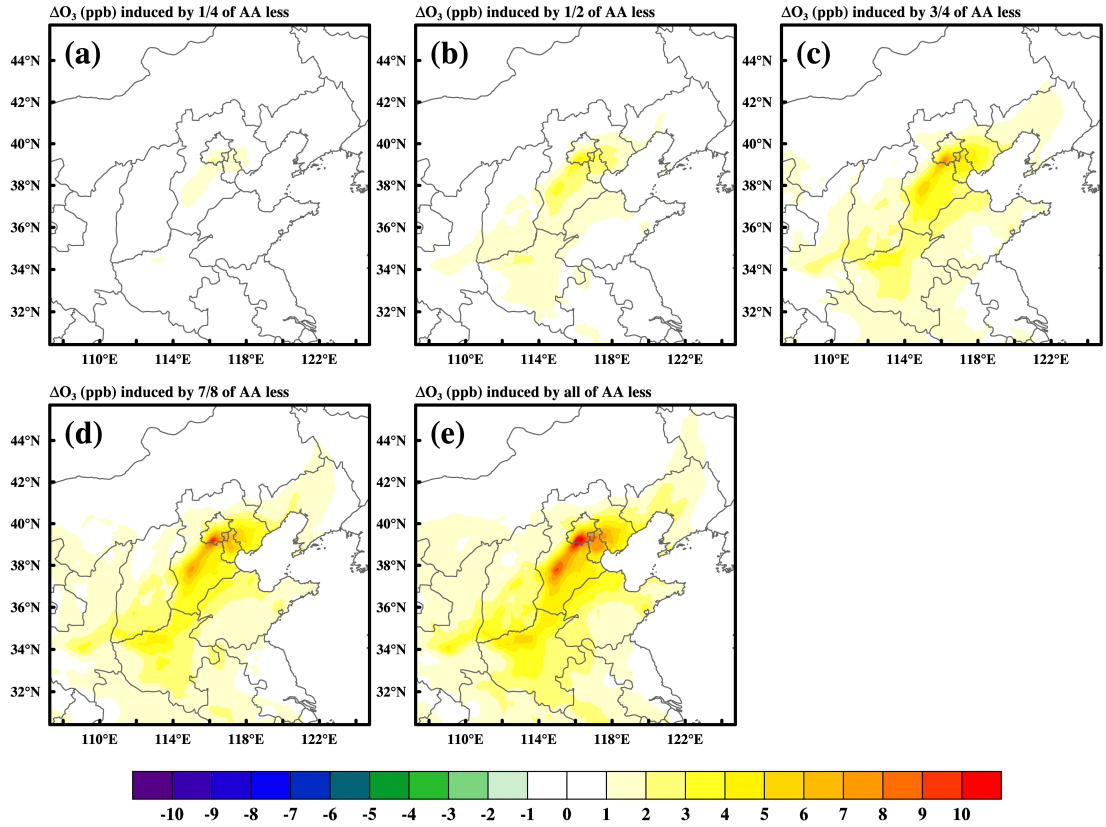

Table S1. Refractive indexes of the aerosol species at each wave band in WRF-Chem model.

wave band	300nm		400nm		600nm		999nm	
refr. index[a] / species	real[b]	imaginary[c]	real	imaginary	real	imaginary	real	imaginary
SO_4	1.52	1.00×10^{-9}	1.52	1.00×10^{-9}	1.52	1.00×10^{-9}	1.52	1.75×10^{-9}
NO_3	1.50	0.00	1.50	0.00	1.50	0.00	1.50	0.00
NH_4	1.50	0.00	1.50	0.00	1.50	0.00	1.50	0.00
Na	1.51	8.66×10^{-7}	1.50	7.02×10^{-8}	1.50	1.18×10^{-8}	1.47	1.50×10^{-4}
Cl	1.51	8.66×10^{-7}	1.50	7.02×10^{-8}	1.50	1.18×10^{-8}	1.47	1.50×10^{-4}
OC	1.45	0.00	1.45	0.00	1.45	0.00	1.45	0.00
BC	1.85	0.71	1.85	0.71	1.85	0.71	1.85	0.71
OIN	1.55	3.00×10^{-3}	1.55	3.00×10^{-3}	1.55	3.00×10^{-3}	1.55	3.00×10^{-3}

[a] refr. index = refractive index; [b] real = real part; [c] imaginary = imaginary part

Table S2. Mean model performance metrics for meteorological factors and air pollutants. Values do not meet the benchmarks are denoted in bold.

Variables	IOA	MB	RMSE	MNB	MFB
T2 (°C)	0.93 (≥0.8)	**0.71** ([-0.5,0.5])	2.42	-0.01	-0.09
WS ($m\ s^{-1}$)	0.78 (≥0.6)	-0.42 ([-0.5,0.5])	1.26 (≤2)	-0.03	-0.28
WD (°)	0.89	6.59 ([-10,10])	-0.42	1.64	0.02
O_3 ($\mu g\ m^{-3}$)	0.84	-6.51	27.68	**0.16** ([-0.15,0.15])	-0.24
NO_2 ($\mu g\ m^{-3}$)	0.73	-5.97	23.39	-0.13	-0.35
$PM_{2.5}$ ($\mu g\ m^{-3}$)	0.74	8.11	28.75	0.34	0.08 ([-0.6,0.6])